Post metallization annealing study in La_2O_3/Ge MOS structure

J. Song [a], K. Kakushima [b], P. Ahmet [a], K. Tsutsui [b], N. Sugii [b], T. Hattori [a], H. Iwai [a]

[a] *Frontier Research Center, Tokyo Institute of Technology, 4259 Nagatsuta, Midori-ku, Yokohama 226-8503, Japan*

[b] *Interdisciplinary Graduate School of Science and Engineering, Tokyo Institute of Technology, 4259 Nagatsuta, Midori-ku, Yokohama 226-8502, Japan*

Abstract

The study on post metallization annealing (PMA) in electrical characteristics and interfacial properties of La_2O_3/Ge structures has been conducted. The PMA treatment in N_2 ambient induces the growth of interfacial Ge oxide layer accompanied with decrease of capacitance value and interface trap density. The interface-layer growth is caused by the oxidation of Ge substrate due to the hydroxyl group absorbed in La_2O_3 from the ambient. The metal electrode capping might prevent the hydroxyl from evaporating during annealing, which enhances the interface reaction. On the other hand, leakage current increment has been observed for the sample with PMA in case of using Pt gate electrode. It is due to the diffusion of Pt and/or Ge and a Pt-germanide formation in La_2O_3 film during PMA. This leakage current increment can be suppressed by using Ta or W electrode which has less reactivity with Ge than Pt at high temperature.

1. Introduction

As the scaling of silicon metal-oxide-semiconductor field-effect transistor (MOSFET) is approaching its fundamental limits, germanium FET has drawn a lot of attention for further performance improvement thanks to its high carrier mobility [1]. Although relatively excellent interfacial properties are reported recently in the MOS structure using the oxide film grown by electron cyclotron resonance plasma oxidation [2], Ge oxide as gate dielectric has some critical problems. The problems include thermodynamically unstable property [3], water solubility and low conduction band offset of 1.04 eV [4]. In addition, considering the technology generation that Ge channel will be used, the achievement of a small equivalent oxide thickness (EOT) is essential. For these reasons, high dielectric constant (high-*k*) materials such as ZrO_2 [5], HfO_2 [6] or rare earth oxides [7-10] are considered to be more advantageous than Ge oxide with dielectric constant of about 5-6 [11-12].

In many high-k materials, La_2O_3, one of rare earth oxides, is more attractive than other high-k materials in terms of high dielectric constant (~27) and large band-gap [13-14], in the bulk state, though. Thus, the electrical and physical properties of La_2O_3 on Si substrate have been extensively studied so far, whereas those on Ge substrate are rare [8-10, 12]. In this paper, we report the effect of post metallization annealing (PMA)

on electrical characteristics and interfacial properties of La_2O_3/Ge structures.

2. Experiments

Ge MOS capacitors were fabricated on n-type Ge(100) wafers with resistivity of 0.1~1.0 Ω-cm. The Ge native oxides were removed by dipping in an HCl/H_2O (1/4) solution followed by rinsing in de-ionized water. After that, a protective Ge oxide layer was formed by the $NH_4OH/H_2O_2/H_2O$ (1/2/20) treatment [15]. The wafers were transferred into an ultrahigh-vacuum (UHV) chamber (~10^{-8} Pa) and annealed at 500 ^oC to remove the protective Ge oxide layer. La_2O_3 films were then deposited by electron-beam evaporation using a La_2O_3 tablet as a source under pressure of ~1×10^{-6} Pa at substrate temperature of 250 ^oC. Post deposition annealing (PDA) was conducted in an N_2 ambient at 300-500 ^oC for 5 minutes followed by platinum (Pt) gate electrode formation. Some samples were subjected to PMA in N_2 ambient at 300-500 ^oC for 5 minutes. Interface trap density (D_{it}) was extracted by conductance method with an LCR meter. The chemical bonding states were analyzed by x-ray photoelectron spectroscopy (XPS) with monochromatic Al $K\alpha$ (1486.7 eV) x-ray source.

3. Electrical characteristics and interfacial properties

Figure 1 shows (a) high frequency capacitance-voltage (C-V) characteristics and (b) interface trap density (D_{it}) of the samples with either PDA or PMA treatments. Capacitors with the PMA treatment showed lower capacitance density and the smaller D_{it} compared to those of capacitors with PDA, especially with the 500 ^{o}C annealing. C-V hysteresis observed in PDA samples could not be suppressed by PMA treatment.

Figure 2 shows Ge*3d* spectra of samples annealed at 400 ^{o}C either with PDA or PMA treatment. The thicknesses of the Pt electrode and the La_2O_3 films were set to 1.5 nm and 2.0 nm, respectively. The spectra related to Ge oxide (GeO_x), at higher binding energy with respect to Ge*3d*, can be deconvoluted into four GeO_x peaks (Ge^{1+}, Ge^{2+}, Ge^{3+} and Ge^{4+}) with energy shifts of 0.8, 1.8, 2.6, and 3.4 eV, respectively [16]. Distinct Ge^{4+} as well as Ge^{3+} peaks were observed for the PMA sample, which is minor in the spectrum for the PDA one. The generation of Ge^{3+} and Ge^{4+} components can be considered to contribute in the improvement in D_{it} at the cost of increasing the capacitance [12].

The source to oxidize the Ge substrate during PMA is considered to be the hydroxyl group absorbed near the surface of La_2O_3 from the ambient, as La_2O_3 has high hygroscopic property [17]. The hydroxyl group can be decomposed during PDA, whereas a capping with gate electrode prevents the hydroxyl from evaporation in the

case of PMA. Since Pt is an inert material, the hydroxyl group in La_2O_3 is thought to be the source to oxidize Ge substrate.

In order to confirm the effect of the absorbed hydroxyl group, vacuum annealing to remove the hydroxyl group was performed *in situ* prior to the Pt electrode deposition. Annealing temperature was set at 250 ^oC, which is the same as the substrate temperature during the La_2O_3 deposition. Fig. 3 shows (a) C-V characteristics and (b) D_{it} in $Pt/La_2O_3/Ge$ structure with and without the *in-situ* vacuum annealing before the Pt electrode deposition. PMA was conducted at 300 ^oC and 500 ^oC in N_2 for 5 minutes. Larger capacitance value was observed for the samples with the vacuum annealing. However, a bulky hump was observed in the C-V curve, which indicates the degradation in D_{it} as shown in Fig. 3-(b). These results suggest that the interfacial GeO_x layer thickness is smaller for the vacuum annealed sample than without.

The interfacial layer growth was further confirmed by XPS analyses as shown in Fig. 4. The thicknesses of Pt electrode and La_2O_3 film and were 1.5 nm and 4.5 nm, respectively. The spectra were normalized by La*5s* peak intensity considering that the photoelectrons of La_2O_3 should be the same with each other because it was deposited simultaneously. A large reduction in GeO_x intensity was observed with *in-situ* vacuum annealing in both cases of PMA at 300 ^oC and 500 ^oC. These results confirm the

suppression of the interfacial GeO_x layer growth by reduction in density of the hydroxyl group in the La_2O_3 film during the vacuum annealing.

4. Germanide formation and its effect on leakage current

Figure 5 shows the gate leakage current density (J_g) for the samples either with PDA or PMA. The leakage current of PMA samples shows larger values than those of PDA samples, which increase with increasing the PMA temperature. Moreover, leakage current is strongly depended on the initial La_2O_3 thickness, which suggests diffusion of Pt metal into the La_2O_3 film. Fig. 6 shows results of angle-resolved XPS analyses for the samples of the Pt(1.5nm)/La_2O_3(2.0nm)/Ge structure after PMA in N_2 at 500 ^oC and the La_2O_3(2.3nm)/Ge structure after PDA in N_2 at 500 ^oC, where those spectra were normalized by Ge$3d_{5/2}$ peak intensity. In case of PMA, the intensity of GeO_x (N_{GeOx}) becomes smaller than that of Ge (N_{Ge}) while decreasing the take-off angle (TOA), which means unoxidized Ge is located on the interfacial GeO_x layer. As the La_2O_3 layer is located on the GeO_x layer from the N_{GeOx} decreaing against the N_{La5s} with decaresing the TOA, the unoxidized Ge might exist in the La_2O_3 film. The diffused Ge atoms in La_2O_3 are thought to take the form of GeO_x as excess oxygen is supplied from hydroxyl group during PMA. Therefore, it is reasonable that the unoxidized Ge on the GeO_x layer

is Pt-germanide formed by diffused Pt and Ge, which spectra have almost same binding energy with Ge*3d*. Thus, we anticipate the diffusion of Ge and/or Pt into the La_2O_3 film and a Pt-germanide reaction in the La_2O_3 film during the PMA are responsible for increasing the leakage current. On the other hand, Pt-germanide peak did not appear in Pt*4f* spectra measured from this sample (not shown). It seems that very little amount of Pt-germanide was formed in the La_2O_3 film and majority part of Pt*4f* spectra were gathered from the surface Pt electrode considering the surface sensitivity of XPS.

The increase in leakage current after PMA treatment can be well suppressed by using tantalum (Ta) or tungsten (W) gate electrode, which is less inert materials than Pt and has high reaction-temperature with Ge [18, 19]. Fig. 7 shows (a) leakage-current characteristics and (b) C-V characteristics in metal/La_2O_3/Ge structures using Pt, Ta, and W as a gate electrode material. Small EOT of 1.2 nm with a leakage current density of 2×10^{-7} A/cm^2 at 1V was achieved by using W electrode after PMA at 300 ^{o}C. Further improvement, however, was not observed in C-V hysteresis and D_{it} with Ta and W gate electrode. Further research is still needed.

5. Conclusion

The effects of post-metallization annealing on electrical characteristics and

interfacial properties for the metal/La_2O_3/Ge structures were investigated. The hygroscopic property of La_2O_3 induces the interfacial Ge oxide layer growth during PMA as a capping gate electrode prevents the absorbed hydroxyl group in La_2O_3 from evaporating during annealing. Removal of hydroxyl group in La_2O_3 prior to deposition of metal electrode can suppress the growth of interfacial Ge oxide layer. On the other hand, PMA samples with Pt electrode show larger leakage current than those of PDA samples. This increase of leakage current in PMA samples is thought to be due to the diffusion of Pt and/or Ge and a Pt-germanide formation during PMA from the XPS results. This leakage current increment by the PMA treatment can be suppressed by using metals such as Ta or W which is less reactive with Ge than Pt at high temperatures.

Acknowledgment

This work was partially supported by Semiconductor Technology Academic Research Center (STARC).

References

[1] T. Tezuka, S. Nakaharai, Y. Moriyama, N. Hirashita, E. Toyoda, N. Sugiyama, T. Mizuno, and S. Takagi, VLSI Symp. Tech. Dig. (2005) 80.

[2] Y. Fukuda, T. Ueno, S. Hirono, and S. Hashimoto, Jpn. J. Appl. Phys. 44 (2005) 6981.

[3] K. Prabhakaran, F. Maeda, Y. Watanabe, and T. Ogino, Appl. Phys. Lett. 76 (2000) 2244.

[4] A. Ohta, H. Nakagawa, H. Murakami, S. Higashi, and S. Miyazaki, e-J. Surf. Sci. Nanotechnol. 4 (2006) 174.

[5] C. O. Chui, H. Kim, D. Chi, B. B. Triplett, P. C. McIntyre, and K. C. Saraswat, Tech. Dig. - Int. Electron Devices Meet. (2002) 437.

[6] W. P. Bai, N. Lu, J. Liu, A. Ramirez, D. L. Kwong, D. Wristers, A. Ritenour, L. Lee, and D. Antoniadis, VLSI Symp. Tech. Dig. (2003) 121.

[7] E. K. Evangelou, G. Mavrou, A. Dimoulas, and N. Konofaos, Solid-State Electron. 51 (2007) 164.

[8] J. Song, K. Kakushima, P. Ahmet, K. Tsutsui, N. Sugii, T. Hattori, and H. Iwai, Jpn. J. Appl. Phys. 46 (2007) L376.

[9] A. Dimoulas, D. P. Brunco, S. Ferrari, J. W. Seo, Y. Panayiotatos, A. Sotiropoulos, T. Conard, M. Caymax, S. Spiga, M. Fanciulli, Ch. Dieker, E. K. Evangelou, S. Galata, M. Houssa, and M. M. Heyns, Thin Solid Films 515 (2007) 6337.

[10] G. Mavrou, S. F. Galata, A. Sotiropoulos, P. Tsipas, Y. Panayiotatos, A. Dimoulas, E. K. Evangelou, J. W. Seo, and Ch. Dieker, Microelectron. Eng. 84 (2007) 2324.

[11] E. B. Gorokhov, I. G. Kosulina, S. V. Pokrovskaya et al., Phys. Stat. Sol. (a) 101 (1987) 451.

[12] J. Song, K. Kakushima, P. Ahmet, K. Tsutsui, N. Sugii, T. Hattori, and H. Iwai, Microelectron. Eng. 84 (2007) 2336.

[13] T. Hattori, T. Yoshida, T. Shiraishi, K. Takahashi, H. Nohira, S. Joumori, K. Nakajima, M. Suzuki, K. Kimura, I. Kashiwagi, C. Ohshima, S. Ohmi, and H. Iwai, Microelectron. Eng. 72 (2004) 283.

[14] A. Chin, Y. H. Wu, S. B. Chen, C. C. Liao, and W. J. Chen, VLSI Symp. Tech. Dig. (2000) 16.

[15] H. Okumura, T. Akane, and S.Matsumoto, Appl. Surf. Sci. 125 (1998) 125.

[16] D. Schmeisser, R.D. Schnell, A. Bogen, F.J. Himpsel, D. Rieger, G. Landgren, and J.F. Morar, Surf. Sci. 172 (1986) 455.

[17] Y. Zhao, M. Toyama, K. Kita, K. Kyuno, and A. Toriumi, Ext. Abstr. SSDM (2005)

546.

[18] O. Yu. Khyzhun, Ya. V. Zaulychny, and E. A. Zhurakovsky, J. Alloys and Compounds 244 (1996) 107.

[19] M. W. Ruckman, M. del Giudice, and J. H. Weaver, Phys. Rev. B 32 (1985) 1077.

List of figure captions

Fig. 1. (a) 100kHz C-V characteristics and (b) D_{it} of the Pt/La_2O_3/Ge structures with PDA or PMA. The gate voltage was swept from inversion to accumulation when the conductance was measured for D_{it} extraction.

Fig. 2. (a) Spectra of Ge*3d* measured by XPS using Pt(1.5nm)/La_2O_3(2.0nm)/Ge structure with PMA at 400 ^{o}C and La_2O_3(2.0nm)/Ge structure with PDA at 400 ^{o}C.

Fig. 3. (a) C-V characteristic and (b) D_{it} in Pt/La_2O_3/Ge structure with and without *in situ* vacuum annealing before Pt electrode deposition.

Fig. 4. XPS spectra of Ge*3d* in Pt/La_2O_3/Ge structure with and without *in situ* vacuum annealing before Pt electrode deposition.

Fig. 5. Leakage current density for the samples with PDA or PMA at various temperatures and for the PMA samples with various thicknesses of La_2O_3 film.

Fig. 6. Angle-resolved XPS analyses in Pt(1.5nm)/La_2O_3(2.0nm)/Ge structure with PMA in N_2 at 500 ^oC and in La_2O_3(2.3nm)/Ge structure with PDA in N_2 at 500 ^oC.

Fig.7. (a) leakage current density and (b) C-V characteristics in metal/La_2O_3/Ge structures using Pt, Ta, and W as a gate electrode. PMA was carried out at 300 ^oC in N_2 for 5 minutes.

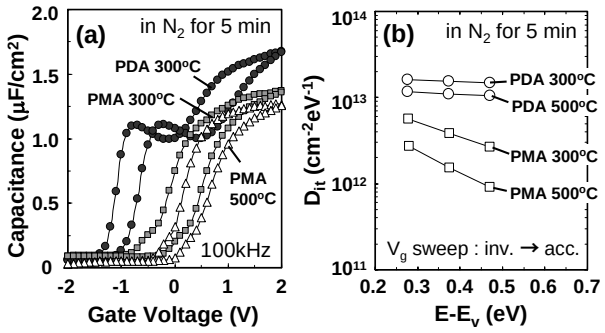
(a)
in N2 for 5 min
PDA 300°C
PMA 300°C
PMA 500°C
100kHz
Capacitance (μF/cm²)
Gate Voltage (V)
(b)
in N2 for 5 min
PDA 300°C
PDA 500°C
PMA 300°C
PMA 500°C
Vg sweep : inv. → acc.
Dit (cm-2eV-1)
E-Ev (eV)

Fig. 1

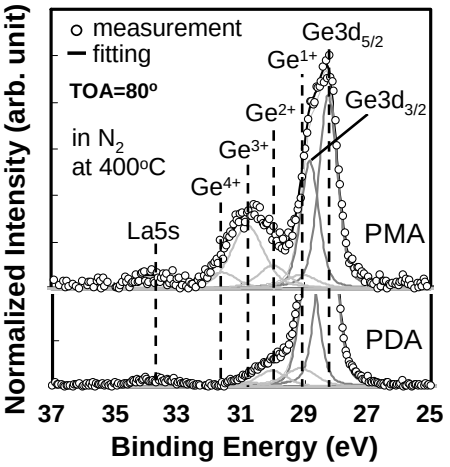
measurement
fitting
TOA=80°
in N2
at 400°C
Ge3d5/2
Ge1+
Ge2+
Ge3+
Ge4+
Ge3d3/2
La5s
PMA
PDA
Normalized Intensity (arb. unit)
37
35
33
31
29
27
25
Binding Energy (eV)

Fig. 2

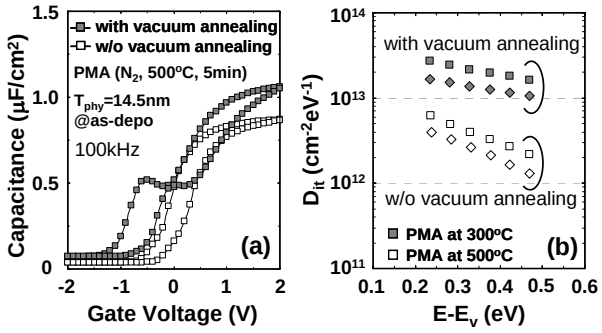
with vacuum annealing
w/o vacuum annealing
PMA (N2, 500°C, 5min)
Tphy=14.5nm
@as-depo
100kHz
(a)
Capacitance (μF/cm²)
Gate Voltage (V)
with vacuum annealing
w/o vacuum annealing
PMA at 300°C
PMA at 500°C
(b)
Dit (cm-2eV-1)
E-Ev (eV)

Fig. 3

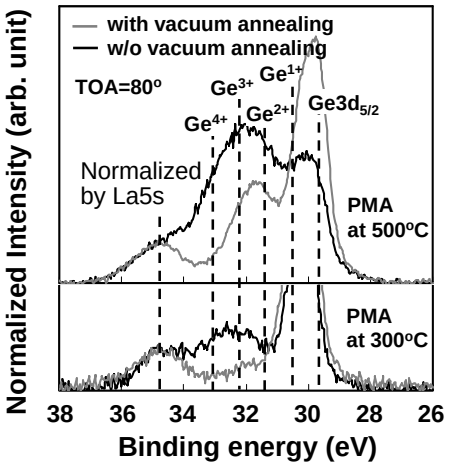
with vacuum annealing
w/o vacuum annealing
TOA=80°
Ge3+
Ge1+
Ge4+
Ge2+
Ge3d5/2
Normalized
by La5s
PMA
at 500°C
PMA
at 300°C
Normalized Intensity (arb. unit)
38
36
34
32
30
28
26
Binding energy (eV)

Fig. 4

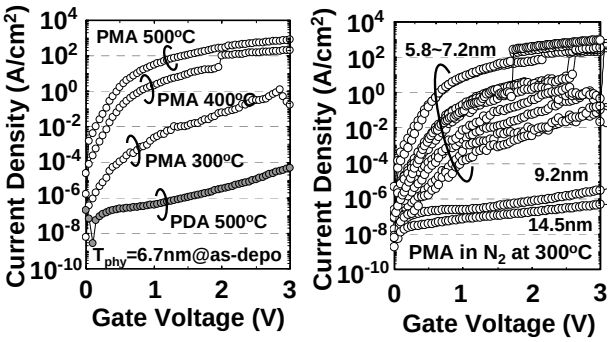
Current Density (A/cm²)
Gate Voltage (V)
PMA 500°C
PMA 400°C
PMA 300°C
PDA 500°C
T_phy=6.7nm@as-depo
5.8~7.2nm
9.2nm
14.5nm
PMA in N2 at 300°C

Fig. 5

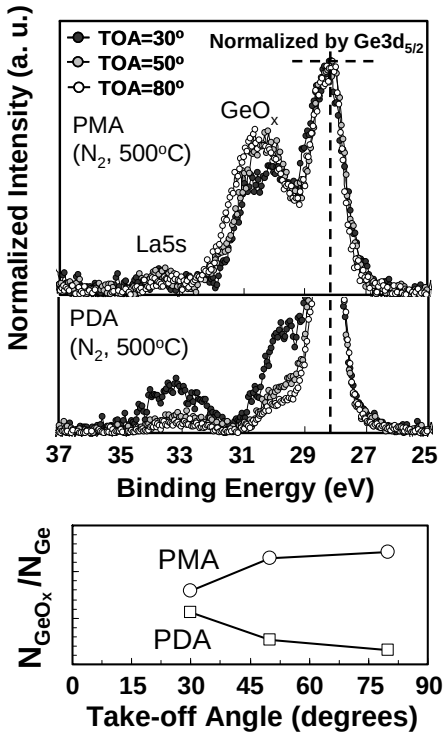
TOA=30º
TOA=50º
TOA=80º
Normalized by Ge3d5/2
GeOx
PMA
(N2, 500ºC)
La5s
PDA
(N2, 500ºC)
Normalized Intensity (a. u.)
37 35 33 31 29 27 25
Binding Energy (eV)
NGeOx/NGe
PMA
PDA
0 15 30 45 60 75 90
Take-off Angle (degrees)

Fig. 6

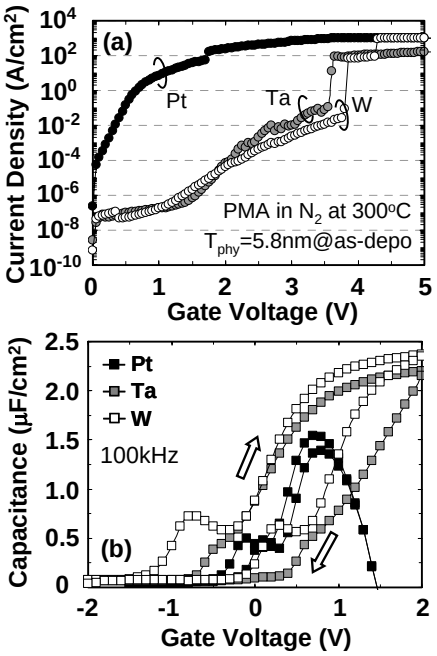
(a)
Pt
Ta
W
PMA in N2 at 300°C
Tphy=5.8nm@as-depo
Current Density (A/cm2)
Gate Voltage (V)
Pt
Ta
W
100kHz
(b)
Capacitance (μF/cm2)
Gate Voltage (V)

Fig. 7